Journal of Intelligent and Robotic Systems (2005) 44: 25–46
DOI: 10.1007/s10846-005-9022-4

Dynamic Analysis of a Nonholonomic Two-Wheeled Inverted Pendulum Robot

YEONHOON KIM*, SOO HYUN KIM and YOON KEUN KWAK
Department of Mechanical Engineering, KAIST, 373-1 Guseong-dong, Yuseong-gu, Daejeon, 305-701, South Korea. E-mail: yeonhoon@kaist.ac.kr, soohyun@kaist.ac.kr, ykkwak@kaist.ac.kr★

(Received: 2 April 2004; in final form: 2 September 2005)

Abstract. As a result of the increase in robots in various fields, the mechanical stability of specific robots has become an important subject of research. This study is concerned with the development of a two-wheeled inverted pendulum robot that can be applied to an intelligent, mobile home robot. This kind of robotic mechanism has an innately clumsy motion for stabilizing the robot's body posture. To analyze and execute this robotic mechanism, we investigated the exact dynamics of the mechanism with the aid of 3-DOF modeling. By using the governing equations of motion, we analyzed important issues in the dynamics of a situation with an inclined surface and also the effect of the turning motion on the stability of the robot. For the experiments, the mechanical robot was constructed with various sensors. Its application to a two-dimensional floor environment was confirmed by experiments on factors such as balancing, rectilinear motion, and spinning motion.

Key Words: dynamic modeling, intelligent robot, inverted pendulum, mobile robot, nonholonomic system, stability.

1. Introduction

Through various applications, robots in the twenty-first century have a social role of leading industries. Robot technology is ubiquitous in various fields; it brings enormous benefits and profit to many nations. In the twentieth century, robots were generally used to aid or replace human labor in factories. Recently, robots have been used in other environments such as the home or office, where they serve as guard robots, service robots, care robots, exploration robots, and entertainment robots. Intelligent robots need a specific mechanism suitable for the specific purpose of the robot. For this reason, we need to research the mechanically stable implementation of each type of mechanism.

Although intelligent robots can be created with various kinds of mechanisms, most mechanisms can be categorized as humanoid or pet robots. Humanoid robots, such as ASIMO, SDR and PINO, are burdened by a highly complex control [1]. However, they are still considered appropriate for an intelligent robot because their external appearance is similar to humans. Mechanisms that resemble

★ This e-mail address is available for all problems and questions.
* Corresponding author.

animals or insects are also frequently adopted because of their human-friendly characteristics, as can be seen in the case of Sony's AIBO [2] and Bandai's BN-1. These animal-type robots have been manufactured and sold already; they have the advantage that they are already intelligent naturally in their shape.

The type of intelligent robot proposed here is a mobile robot with a two-wheeled inverted pendulum. This design was chosen because its mechanism has an innately clumsy motion for stabilizing the robot's body posture. The robot has a body with two wheels for moving in a plane and a head similar to a human head for controlling the motion. Two independent driving wheels are used for position control, for fast motion in a plane without casters, and for some actions that help the robot appear to be intelligent.

We use a two-wheeled inverted pendulum-type mobile robot as an intelligent robot and we investigate the detailed dynamics of this robotic mechanism. In Section 2, we introduce the features of this type of robotic mechanism from a dynamical point of view. In Section 3, we discuss the detailed dynamics of the robot with the aid of 3-DOF modeling, along with the relevant issues from the governing equations and the challenges that this type of mobile robot presents. In Section 4, we describe the design of the robotic mechanism and the sensor system used in the experiments. In Section 5, we discuss the strategy and control scheme of the robot's motions. We also present the experimental results of the basic motions with graphical results.

2. Two-wheeled inverted pendulum robot

2.1. INTRODUCTION OF THE ROBOT

Several kinds of wheels can be attached to the wheeled mobile robot, but they fall into one of two categories: driving wheels or auxiliary wheels. The driving wheels are rotated to permit the robot to move when torque is applied to the axles. The auxiliary wheels merely ease the movement of the robot and enable its body to be suspended when no torque is applied to the axles. In most wheeled mobile robots at least one wheel is an auxiliary wheel.

Auxiliary wheels can be classified as either a centered orientable wheel or an off-centered orientable wheel (the so-called caster wheel). Although the centered orientable wheel can be steered, the robot's motion is restricted because the wheel cannot normally move in a vertical direction. This restriction contrasts with the off-centered orientable wheel, which is omnidirectional. The off-centered orientable wheel can move freely in any direction whereas the centered orientable wheel cannot move freely. Because of this omnidirectional feature, the off-centered orientable wheel is considered a more effective auxiliary wheel. The wheels on a shopping trolley are a good example of this kind of wheel.

Auxiliary wheels must move smoothly without causing the robot to be interrupted. In office chairs, for instance, wheels are popular because they make

it easy to move around. This motion can be easily performed by using bearings in the axles and by running the wheels on a smooth surface without a heavy load. Sometimes, however, the wheels do not work. Even in an office environment where the surface is normally very smooth, the wheels frequently slide or slip when the chairs are dragged, though they were designed to roll without sliding or slipping. Furthermore, the ideal performance of auxiliary wheels is more difficult to attain on a hard or rugged surface. These problems occur in every object equipped with auxiliary wheels, including wheeled mobile robots. To overcome these problems, we need to improve the operation of auxiliary wheels or, alternatively, to replace them with something different.

The same thing applies to two-wheeled mobile robots, which commonly have only one centered or off-centered orientable wheel. For a two-wheeled mobile robot, we can ask what would happen if the auxiliary wheels were removed altogether instead of being replaced with something different or instead of improving the performance of the wheels.

By getting rid of the auxiliary wheels, the number of wheels attached on the robot would be reduced. Moreover, the mechanical characteristic of the robot would be completely altered because no elements could suspend and balance the robot's body except for the driving wheels. That is, the robot would have to move and balance its body with only two driving wheels.

The mechanical structure of a robot with only two driving wheels is similar to an inverted pendulum. Compared to common inverted pendulums, the two-wheeled inverted pendulum robot has different, complicated problems. Hence, we need to investigate its mechanical characteristics and determine whether this type of robot is a valid proposal. First, we need to construct the exact dynamics of the proposed structure and show that it can control the robot. We also need to clarify its strong points and weak points from the viewpoint of energy, control and dynamics. Finally, we need to determine if the system has commercial applicability or is purely for academic purposes.

2.2. PREVIOUS RESEARCH

Those processing fewer actuators than degrees of freedom are underactuated systems. Two-wheeled inverted pendulum robot has just two driving wheels for actuator. However, it has three degrees of freedom; two of planar motions and one of tilt-angular motion. And the dynamics are nonlinear as appeared in next chapter. So we can say it an underactuated system and that it is nonlinear. The previous work for those concerns are researched many times, however the applications were restricted as free-flying robots, snake-like robots or crawling robots [3–5]. As a viewpoint of tilt-up control, Au et al. researched gyroscopically stabilized robot [6] and Awtar et al. have studied inverted pendulum systems [7]. Deniskina et al. proposed a common sense solution to the stability problem and applied it to human postural control [8]. However, their systems are not exactly

same with the inverted pendulum robot driving by only two wheels. So, dynamics, control systems and the related analysis should be executed with this kind of mechanical system.

Several studies purely on the two-wheeled inverted pendulum robot have been undertaken. In 1989, Yamafuji and Kawamura built a 1-DOF model that focused solely on the tilt angle and they conducted experiments based on Routh–Hurwitz stability [9]. In 1996, Ha and Yuta proposed another inverted pendulum–type, self-contained mobile robot [10]. With a driving wheel on each side of its body and no other supporting wheels, it could navigate autonomously in a plane while keeping its own balance at a relatively high speed. In 2000, Segway™ developed a human transporter whose speed and direction were controlled by the shifting weight of the rider and a manual turning mechanism on one of its handlebars [11–13]. Segway implemented a PID controller for its vehicle, but the difference between their control system and that proposed by Ha and others is slight, even though the mechanical makeup is not identical. Above researches are about two-wheeled inverted pendulum, but with a different motivation from this study. Those studies were started out of a curiosity to know whether the two-wheeled inverted pendulum robot could be realized in practice.

In 2002, Grasser et al. presented an inverted pendulum mobile robot [14] whose mechanical constitution and control system were similar to that of the research of Ha. Compared with other studies, they constructed a more advanced mathematical model to describe the dynamics, whereas other researchers constructed a simplified, one-dimensional model. However, they have also mainly focused on the control system to define the equations of motion. Their treatment in dynamics implicitly assumed that the rotational motion of the wheels around the axis in the direction of gravity is negligible. To make such assumption valid, the wheels are to be designed to have relatively small rotational inertia to the direction of gravity.

Although above works summarized in this section have a slightly different mechanical structure and control system, all of them show the practical validity of the robot that means the robot is controllable actually. However, concerns about the dynamics of this kind of robot have not been studied. We therefore investigated the exact dynamics because the dynamics will provide important information that will be helpful for further design and production. When it is applied to the control, the dynamics will show its exactness and correctness. The characteristics and application of this kind of robot must then be studied.

3. Dynamics of the robot

Development of a dynamic model is important for comprehending the physical phenomenon of a robot and for modifying the system of the robot. In addition, a

dynamic model should be developed so that the robot can smoothly generate proper motions. For manipulation of motion, we need to know kinematical information such as velocities and angular speeds; the motion equations will also be used widely when they are applied to the control scheme.

Figure 1 describes two-wheeled inverted pendulum robot that we constructed. Although several studies investigated two-wheeled inverted pendulum robots, they failed to emphasize the exact dynamics. To develop a dynamic model, we used Kane's method [15]. The coordinate system for the robot is described in Figure 2. And the definitions of some important mechanical parameters are listed in Table I. We set F as the Newtonian reference frame, S as the main body, C_1 as the left and C_2 as the right wheel. We defined the unit vectors $\mathbf{n_1}$, $\mathbf{n_2}$, $\mathbf{n_3}$ on the central point of the line between the two wheels.

3.1. NONHOLONOMIC SYSTEM AND ASSUMPTION

The designed system was assumed to be a nonholonomic system in which no slip occurs between the wheels and the ground. Suppose the configuration of a system is specified by the n generalized coordinates $q_1, q_2, \ldots, q_n$ and assume that there are k independent equations of constraint of the form [16]

$$\varphi_j = (q_1, q_2, \ldots, q_n) = 0 \quad (j = 1, 2, \ldots, k) \tag{1}$$

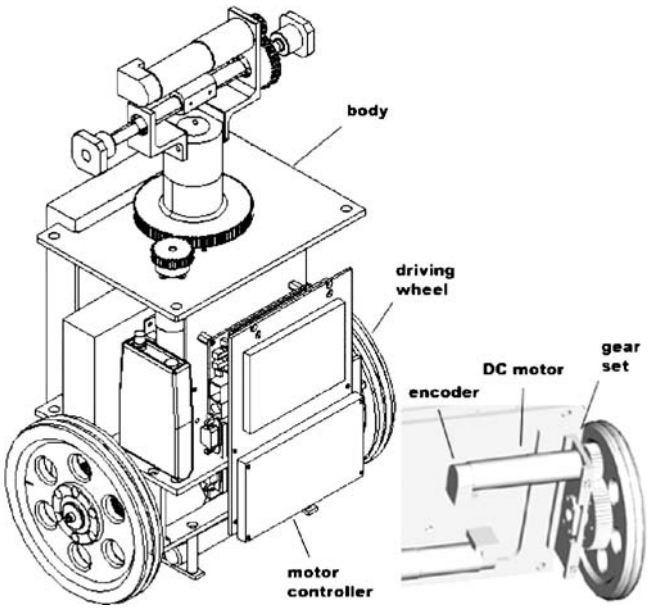

Figure 1. Two-wheeled inverted pendulum robot.

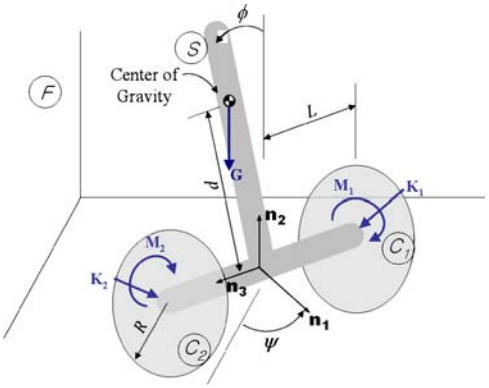

Figure 2. Coordinate system of the robot and assumption of exerted forces.

A constraint which can be expressed in this fashion is known as a holonomic constraint. On the contrary, let us consider a system of m constraints, which are written as nonintegerable differential expressions of the form

$$\sum_{i=1}^{n} a_{ji}\dot{q}_i + a_{jt} = 0 \quad (j = 1, 2, \ldots, m) \tag{2}$$

where the as are, in general, functions of the qs. Constraints of this type are known as nonholonomic constraints.

The nonholonomic constraint which explains why the wheels do not slip on the ground is expressed in Equation (3). After considering it, the generalized speeds, u_i, for Kane's method can be defined in Equation (4) as follows:

$$^{F}\mathbf{v}^{\widehat{C_1}} = {}^{F}\mathbf{v}^{\widehat{C_2}} = \mathbf{0} \tag{3}$$

$$\begin{aligned} u_1 &= \dot{x} = {}^{F}\mathbf{v}^{S_C} \cdot \mathbf{n_1} \\ u_2 &= \dot{\psi} = {}^{F}\boldsymbol{\omega}^{S} \cdot \mathbf{n_2} \\ u_3 &= \dot{\phi} = {}^{F}\boldsymbol{\omega}^{S} \cdot \mathbf{n_3} \end{aligned} \tag{4}$$

Table I. Important mechanical parameters.

Body	
d, distance from C to C.G.	0.1 m
m_s, mass of the body	4.315 kg
I_2, $\mathbf{n_2}$-directional rotational inertia of the body	3.679×10^{-3} kg m^2
I_3, $\mathbf{n_3}$-directional rotational inertia of the body	28.07×10^{-3} kg m^2
L, half-distance between wheels	0.1 m
Wheel	
R, radius of the wheel [m]	0.073
m_c, mass of the wheel [kg]	0.503

The exerted forces on the robot system are assumed to be the forces and torques between the wheels and body of the driving motors, and the gravitational force on the center of gravity of the main body as described in Figure 2. These forces are assumed as follows:

$$\begin{aligned}
\mathbf{K}_1 &= \gamma_1 \mathbf{n_1} + \gamma_2 \mathbf{n_2} + \gamma_3 \mathbf{n_3} \\
\mathbf{K}_2 &= \delta_1 \mathbf{n_1} + \delta_2 \mathbf{n_2} + \delta_3 \mathbf{n_3} \\
\mathbf{M}_1 &= \alpha_1 \mathbf{n_1} + \alpha_2 \mathbf{n_2} + n_3 \mathbf{n_3} \\
\mathbf{M}_2 &= \beta_1 \mathbf{n_1} + \beta_2 \mathbf{n_2} + \beta_3 \mathbf{n_3} \\
\mathbf{G} &= -m_S g \mathbf{n_2}
\end{aligned} \tag{5}$$

where **K**s are forces exerted on wheels and **M**s are torques generated by motors on wheels, **G** is gravitational force of body.

3.2. KINEMATICS OF THE ROBOT

The velocities, accelerations, angular velocities and angular accelerations for each part are considered as types of generalized speeds, u_i. Firstly, the angular velocity of the body and the velocity at the center of gravity in the body are governed as follows:

$$\begin{aligned}
{}^F\boldsymbol{\omega}^S &= u_2 \mathbf{n}_2 + u_3 \mathbf{n}_3 \\
{}^F\mathbf{v}^{S^C} &= u_1 \mathbf{n}_1 \\
{}^F\mathbf{v}^{S^*} &= {}^F\mathbf{v}^{S^C} + {}^F\boldsymbol{\omega}^S \times \mathbf{d} \\
&= (u_1 - u_3 d \cos\phi)\mathbf{n}_1 - u_3 d \sin\phi \mathbf{n}_2 + u_2 d \sin\phi \mathbf{n}_3.
\end{aligned} \tag{6}$$

The angular velocities of each wheel and the velocity at the center of each wheel are governed as follows:

$$\begin{aligned}
{}^F\boldsymbol{\omega}^{C_1} &= \left(-\frac{1}{R}u_1 + \frac{L}{R}u_2\right)\mathbf{n}_3 + u_2 \mathbf{n}_2 \\
{}^F\mathbf{v}^{C_1^*} &= (u_1 - u_2 L)\mathbf{n}_1
\end{aligned} \tag{7}$$

$$\begin{aligned}
{}^F\boldsymbol{\omega}^{C_2} &= \left(-\frac{1}{R}u_1 - \frac{L}{R}u_2\right)\mathbf{n}_3 + u_2 \mathbf{n}_2 \\
{}^F\mathbf{v}^{C_2^*} &= (u_1 - u_2 L)\mathbf{n}_1
\end{aligned} \tag{8}$$

The angular accelerations for each left and right wheel are governed as follows:

$$
\begin{aligned}
{}^F\boldsymbol{\alpha}^S &= \dot{u}_2\mathbf{n}_2 + \dot{u}_3\mathbf{n}_3 \\
{}^F\boldsymbol{\alpha}^{C_1} &= \left(-\tfrac{1}{R}u_1u_2 + \tfrac{L}{R}u_2^2\right)\mathbf{n}_1 + \dot{u}_2\mathbf{n}_2 \\
&\quad + \left(-\tfrac{1}{R}\dot{u}_1 + \tfrac{L}{R}\dot{u}_2\right)\mathbf{n}_3 \\
{}^F\boldsymbol{\alpha}^{C_2} &= \left(-\tfrac{1}{R}u_1u_2 - \tfrac{L}{R}u_2^2\right)\mathbf{n}_1 \\
&\quad + \dot{u}_2\mathbf{n}_2 \\
&\quad + \left(-\tfrac{1}{R}\dot{u}_1 - \tfrac{L}{R}\dot{u}_2\right)\mathbf{n}_3
\end{aligned}
\tag{9}
$$

The acceleration of the robot's body and the acceleration at the center of each wheel are governed as follows:

$$
\begin{aligned}
{}^F\mathbf{a}^{S^*} &= \frac{d^F\mathbf{v}^{S_C}}{dt} + {}^F\boldsymbol{\alpha}^S \times \overline{S^CS^*} + {}^F\boldsymbol{\omega}^S \times \left({}^F\boldsymbol{\omega}^S \times \overline{S^CS^*}\right) \\
&\quad \dot{u}_1 - \dot{u}_3 d\ \cos\ \phi + \left(u_2^2 + u_3^2\right) d\ \sin\ \phi \quad \mathbf{n}_1 \\
&= -\dot{u}_3 d\ \sin\ \phi - u_3^2\ d\ \cos\ \phi \quad \mathbf{n}_2 \\
&\quad + \dot{u}_2 d\ \sin\ \phi + u_2u_3\ d\ \cos\ \phi \quad \mathbf{n}_3 \\
{}^F\mathbf{a}^{C_1^*} &= \frac{d^F\mathbf{v}^{S_C}}{dt} + {}^F\boldsymbol{\alpha}^{S_C} \times \overline{S^CC_1^*} + {}^F\boldsymbol{\omega}^{S_C} \times \left({}^F\boldsymbol{\omega}^{S_C} \times \overline{S^CC_1^*}\right) \\
&\quad \dot{u}_1 - L\dot{u}_2 \quad \mathbf{n}_1 \\
&= +0 \quad \mathbf{n}_2 \\
&\quad + Lu_2^2 \quad \mathbf{n}_3 \\
{}^F\mathbf{a}^{C_2^*} &= \frac{d^F\mathbf{v}^{S_C}}{dt} + {}^F\boldsymbol{\alpha}^{S_C} \times \overline{S^CC_2^*} + {}^F\boldsymbol{\omega}^{S_C} \times \left({}^F\boldsymbol{\omega}^{S_C} \times \overline{S^CC_2^*}\right) \\
&\quad \dot{u}_1 + L\dot{u}_2 \quad \mathbf{n}_1 \\
&= +0 \quad \mathbf{n}_2 \\
&\quad - Lu_2^2 \quad \mathbf{n}_3
\end{aligned}
\tag{10}
$$

3.3. EQUATIONS OF MOTION

Using the kinematical information already obtained, we can obtain the generalized active forces and the generalized inertia forces. In the Newtonian

reference frame F, the nonholonomic generalized active forces are constructed with the following equation:

$$\widetilde{F}_r = \sum_{i=1}^{3} \widetilde{\mathbf{v}}_r^{P_i} \cdot \mathbf{R}_i \quad (r = 1, 2, 3) \tag{11}$$

The nonholonomic generalized inertia forces can be obtained as follows:

$$\widetilde{F}_r^* = \sum_{i=1}^{3} \left(\widetilde{\omega}_r^{P_i} \cdot \mathbf{T}_i^* + \widetilde{\mathbf{v}}_r^{P_i} \cdot \mathbf{R}_i^* \right) \quad (r = 1, 2, 3)$$

where (12)

$$\mathbf{R}^* = -M\mathbf{a}^*$$

$$\mathbf{T}^* = -\boldsymbol{\alpha} \cdot \mathbf{I} - \boldsymbol{\omega} \times \mathbf{I} \cdot \boldsymbol{\omega}$$

Finally, the equations of motion in Equation (14) are governed by the relationship in Equation (13) as follows:

$$\widetilde{F}_r + \widetilde{F}_r^* = 0 \quad (r = 1, 2, 3) \tag{13}$$

$$\begin{aligned} &3(m_c + m_s)\ddot{x} - m_s d \cos\phi \ddot{\phi} + m_s d \sin\phi \left(\dot{\phi}^2 + \dot{\psi}^2\right) = -\frac{\alpha_3 + \beta_3}{R} \\ &\left\{\left(3L^2 + 1/2R^2\right)m_c + m_s d^2 \sin^2\phi + I_2\right\}\ddot{\psi} + m_s d^2 \sin\phi \cos\phi \dot{\psi}\dot{\phi} = \frac{L}{R}(\alpha_3 - \beta_3) \\ &m_s d \cos\phi \ddot{x} + \left(-m_s d^2 - I_3\right)\ddot{\phi} + m_s d^2 \sin\phi \cos\phi \dot{\phi}^2 + m_s g d \sin\phi = \alpha_3 + \beta_3 \end{aligned} \tag{14}$$

3.4. CONSIDERATION OF AN INCLINED SURFACE

Although robots generally move on a flat surface with a uniform altitude, we analyzed how a robot would cope with an inclined surface. On an inclined surface, the robot has to deal with the two critical postures shown in Figure 3. From the longitudinal posture of Figure 3(a), we considered the permissible limit of the inclination angle from the viewpoint of the stable posture. And from the lateral posture of Figure 3(b), we investigated how much additional torque is to be needed in the control motor at each inclination angle.

Based on the geometric relation described in Figure 3(a), the maximally permitted inclination angle ξ was decided as follows:

$$\xi \leq \tan^{-1} \frac{L}{d + R} \tag{15}$$

For example, if a robot is designed with $d = 0.1$, $L = 0.1$, and $R = 0.073$, then, to prevent the robot from falling on the floor, the maximum inclined angle cannot exceed 30°.

With respect to an inclined surface, the worst situation for a robot occurs when the robot stands directly toward the lateral line of the inclined surface. To compare

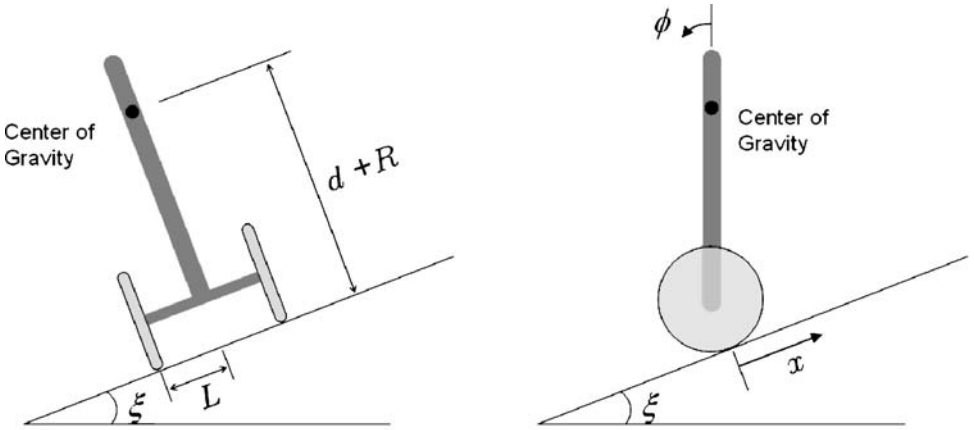

Figure 3. Critical robot postures on the inclined surface.

a flat surface and an inclined surface, we considered the equations with 2-DOF modeling for each situation. To begin with it, the equations of motion for a 2-DOF model of a flat surface are governed by simplifying a 3-DOF model as follows:

$$\begin{aligned}(3m_c + m_s)\ddot{x} - m_s d\cos\phi\ddot{\phi} + m_s d\sin\phi\dot{\phi}^2 &= -\frac{\alpha_3 + \beta_3}{R} \\ - m_s d\cos\phi\ddot{x} + \left(m_s d^2 + I_3\right)\ddot{\phi} - m_s g d\sin\phi &= -\alpha_3 - \beta_3\end{aligned} \tag{16}$$

The Coriolis force and the terms related to steering motion disappeared. With respect to the inclined surface, the equations of motion for the 2-DOF model are governed as follows:

$$\begin{aligned}&(3m_c + m_s)\ddot{x} - m_s d\cos(\phi - \xi)\ddot{\phi} + m_s d\sin(\phi - \xi)\dot{\phi}^2 + (m_c + m_s)g\sin\xi \\ &\quad = -\frac{\alpha_3 + \beta_3}{R} \\ &\quad - m_s d\cos(\phi - \xi)\ddot{x} + \left(m_s d^2 + I_3\right)\ddot{\phi} - m_s g d\sin(\phi - \xi) = -\alpha_3 - \beta_3\end{aligned} \tag{17}$$

A comparison of the two sets of equations of motion shows that, to control the position, x, the robot needs more forces as amount of $(m_c + m_s)g \sin \xi$ increases, and the sinusoidal terms are changed to the functions of $\phi - \xi$ from the functions of ϕ.

We investigated the amount of torque required to control the balancing posture with respect to the inclination of the surface. For doing this, we simulated with the robot parameters that will be introduced in the next chapter. As described in Figure 4, the torque that the motor needed to generate to control remained the same until the inclination angle of the surface went to about 5°. However, when over that range, the required amount of torque increased linearly.

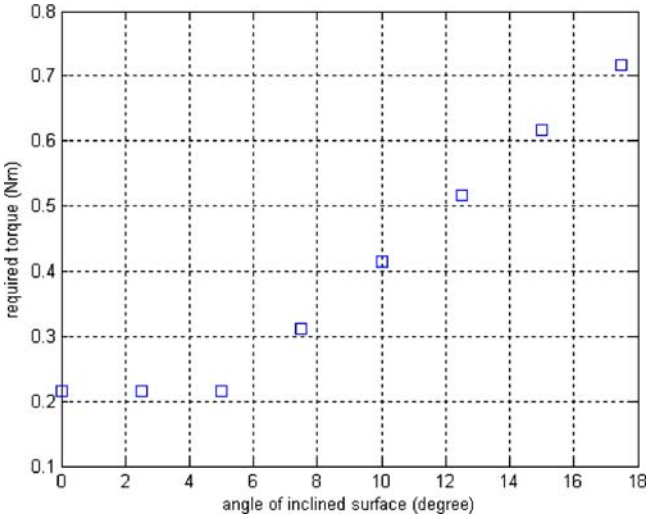

Figure 4. The required torque in simulation w.r.t. the angle of the inclined surface.

Because the rate of increase in graph is high, even with a reduction in gears, a more high-powered motor is needed to cope with inclination surface over 5°.

3.5. EFFECT OF THE TURNING

Equation (14) of the governed motion describes the rectilinear motion, the turning motion, and the tilt motion of the robot line by line. Each variable, along with its derivatives, is placed next to each part of the equation and coupled to affect the other variables. However, as described in the second line of Equation (14), the turning motion less affects the other lines of the equation than the other types of motion do.

We investigated the overshoot of the tilt angle when the robot is controlled under several conditions of $\dot{x}_{ref}$ and $\dot{\psi}_{ref}$. Because, we can say that the effect of turning on dynamics is small if the correlation of the overshoot and $\dot{\psi}_{ref}$ is small. To do this, we simulated the upright control. In Figure 5, the overshoot almost does not increase as the direction of $\dot{\psi}_{ref}$. The turning angular velocity does not have many effects on the stable control of the robot. The increase of the reference velocity has more influence to the control stability as the figure describes the increase in the overshoot of the tilt angle.

4. Fabrication of the robot

4.1. CONSTRUCTION OF THE ROBOT SYSTEM

As early shown in Figure 1, the two-wheeled inverted pendulum robot comprises a main body, gear sets, drive wheels, motors, motor controllers, feedback

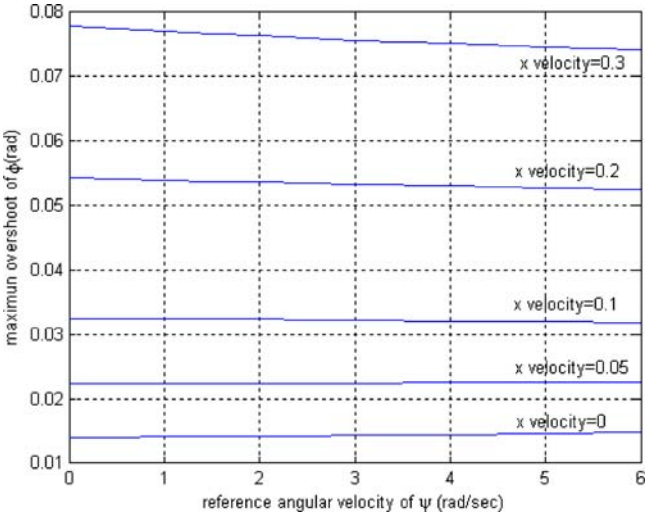

Figure 5. Overshoot of tilt angle ϕ in simulation with the variation of $\dot{x}_{ref}$ and $\dot{\psi}_{ref}$.

sensors, and a PC. The main body is made of aluminum plates and bars, and it has enough space for the necessary electronic boards and sensors. The body is equipped with two DC motors, and the gears of the motors are in contact with the gears of the wheels on the right and left sides. The motors are powered by a battery attached on the bottom of the robot and they are controlled by the motion control processor. Two incremental encoders were used to monitor the behavior of the motors. In addition to the two encoders, a gyroscope and a tilt sensor are mounted on the body of the robot to measure the inclination angle of the body and its time derivative. All these parts constitute the robot, and the PC host controls them. The important mechanical parameters of the robot are listed in Table I.

4.2. THE FEEDBACK SENSORS

In selecting the sensors, we considered the resolution, bandwidth, linear range, sensitivity, and size; the details are listed in Table II. In practice, the physical measurement of a control system is normally detected with a feedback sensor and its derivative or integration is then calculated from that detection. For an inverted pendulum-type system, a gyroscope whose output signal is proportional to the

Table II. Specification of the feedback sensors.

Specification	Tilt sensor	Gyroscope
Linear range	±20°	±80°/s
Resolution	0.05° rms	0.1°/s
Sensitivity	35 mV/°	20.4 mV/°/s
Bandwidth	125 Hz	7 Hz
Size	$1.91 \times 4.763 \times 2.54$ cm^3	$3.7 \times 4.6 \times 1.85$ cm^3

angular velocity is most widely used, and a numerical calculation loop is implemented to enable its integration. However, the numerical integration of the gyroscope output can imply drift error. Thus, in our control system, we independently used the tilt sensor and gyroscope to measure the tilt angle and angular velocity of the robot's body.

4.3. THE MOTOR SYSTEM

The DC motors were connected to the drive wheels to provide the torque to the axles for the upright balancing and navigation of the vehicle. Thus, on the basis of the information provided by the initial hand calculation, we equipped both driving axles with two 11 W motors. Because that calculation proceeded the major dynamic analysis, we used a simplified one-dimensional inverted pendulum model. In such a model, the upright balancing would need much more torque or energy than the steering or posture control.

Between the wheel and the motor, a gear set with a 68:1 reduction ratio was used to offer higher torque to the wheel. Although the dynamic characteristic of backlash that occurs in the gear trains could affect the dynamics of the robot, we assumed it would have an insignificant effect.

5. Experiments

5.1. DESIGN OF THE CONTROLLER

We conducted simulations and experiments to show the feasibility and performance of the proposed robot and to prove the exactness of the derived dynamics. Furthermore, to construct the control system without relying solely on empirical data and trial and error, we applied our theoretical dynamic model to govern the entire system. The dynamic model in Equation (14) that we derived earlier was linearized for the linear feedback control. At zero of tilt angle, the robot system has its quasi-equilibrium state. So we could develop the linearized model under the assumptions that the variation of the tilt angle is small enough to be neglected. Then we have the linearized three equations of motion on the equilibrium state as follows:

$$\ddot{x} = \frac{m_s^2 d^2 g}{3m_c I_3 + 3m_c m_s d^2 + m_s I_3}\phi - \frac{(m_s d^2 + I_3)/R + m_s d}{3m_c I_3 + 3m_c m_s d^2 + m_s I_3}(\alpha_3 + \beta_3) \tag{18}$$

$$\ddot{\psi} = \frac{2L/R}{6m_c L^2 + m_c R^2 + 2I_2}(\alpha_3 - \beta_3) \tag{19}$$

$$\ddot{\phi} = \frac{m_s dg(3m_c + m_s)}{3m_c I_3 + 3m_c m_s d^2 + m_s I_3}\phi - \frac{m_s d/R + 3m_c m_s}{3m_c I_3 + 3m_c m_s d^2 + m_s I_3}(\alpha_3 + \beta_3) \tag{20}$$

After linearization, we rearranged it as the state-space form in Equations (21) and (22), where the state vector and the control input are defined as in Equation (23), the matrices **A** and **B** can be identified as in Equations (24) and (25), the matrix **C** is defined as a 6 × 6 identity matrix and matrix **D** is defined as a 2 × 6 zero-matrix. Equations (21) to (25) are written as follows:

$$\dot{\mathbf{x}} = \mathbf{A}\mathbf{x} + \mathbf{B}\mathbf{u} \tag{21}$$

$$\mathbf{y} = \mathbf{C}\mathbf{x} + \mathbf{D}\mathbf{u} \tag{22}$$

$$\mathbf{x} = \begin{bmatrix} x & \dot{x} & \psi & \dot{\psi} & \phi & \dot{\phi} \end{bmatrix}^t \cdot \mathbf{u} = [\alpha_3 \quad \beta_3]^t \tag{23}$$

$$\mathbf{A} = \begin{bmatrix} 0 & 1 & 0 & 0 & 0 & 0 \\ 0 & 0 & 0 & 0 & \frac{m_s^2 d^2 g}{3m_c I_3 + 3m_c m_s d^2 + m_s I_3} & 0 \\ 0 & 0 & 0 & 1 & 0 & 0 \\ 0 & 0 & 0 & 0 & 0 & 0 \\ 0 & 0 & 0 & 0 & 0 & 1 \\ 0 & 0 & 0 & 0 & \frac{m_s dg(3m_c + m_s)}{3m_c I_3 + 3m_c m_s d^2 + m_s I_3} & 0 \end{bmatrix} \tag{24}$$

$$\mathbf{B} = \begin{bmatrix} 0 & 0 \\ \frac{-(m_s d^2 + I_3)/R - m_s d}{3m_c I_3 + 3m_c m_s d^2 + m_s I_3} & \frac{-(m_s d^2 + I_3)/R - m_s d}{3m_c I_3 + 3m_c m_s d^2 + m_s I_3} \\ 0 & 0 \\ \frac{2L/R}{6m_c L^2 + m_c R^2 + 2I_2} & \frac{-2L/R}{6m_c L^2 + m_c R^2 + 2I_2} \\ 0 & 0 \\ \frac{-m_s d/R - 3m_c m_s}{3m_c I_3 + 3m_c m_s d^2 + m_s I_3} & \frac{-m_s d/R - 3m_c m_s}{3m_c I_3 + 3m_c m_s d^2 + m_s I_3} \end{bmatrix} \tag{25}$$

After conducting the linearization and the test of the controllability and observability, we constructed the overall control scheme. As shown in Figure 6, the tilt sensor, gyroscope, and digital encoder measured six variables: the tilt angle and its time derivative, and the rotation angle and its time derivative for each of the two drive wheels. These values were fed back to the controller. The

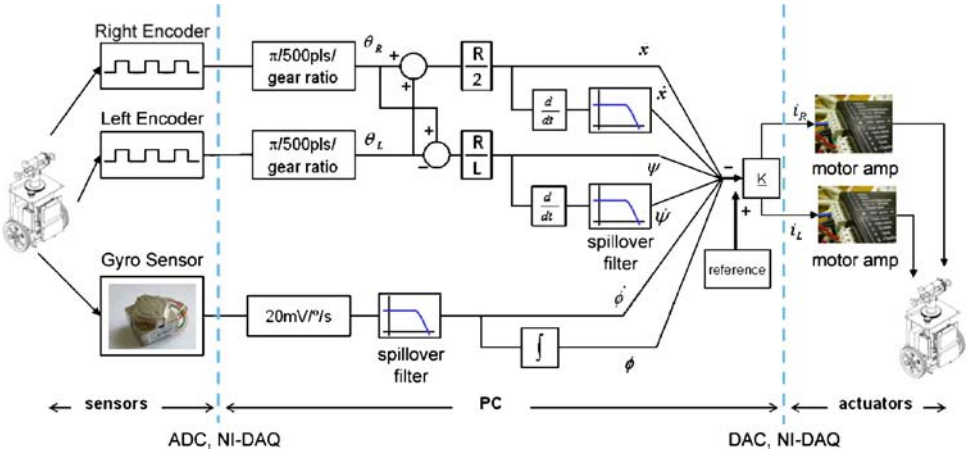

Figure 6. Overall control scheme.

controller computes the state variables from the six feedback values and produces the control input to stabilize and navigate the robot by multiplying the feedback gains and the value of the feedback variables minus the reference values. The computed torque is then decoupled and modified to the actual torque to be applied to the right and left-drive wheels.

To earn the control gain $\mathbf{u} = -\mathbf{Kx}$ for the linear quadratic control, we applied the performance index J and used the solution of the Matrix Riccati equation as follows:

$$J = \int_0^T (\mathbf{x}'\mathbf{Q}\mathbf{x} + u'\mathbf{R}\mathbf{u})dt \tag{26}$$

$$\mathbf{K} = \mathbf{R}^{-1}\mathbf{B}'\mathbf{P} \tag{27}$$

$$-\dot{\mathbf{P}} = \mathbf{A}'\mathbf{P} + \mathbf{P}\mathbf{A} + \mathbf{Q} - \mathbf{P}\mathbf{B}\mathbf{R}^{-1}\mathbf{B}'\mathbf{P} \tag{28}$$

where $\mathbf{Q}$ and $\mathbf{R}$ should be selected. In general, a simple guideline is to select these matrices to be diagonal and to make the diagonal entry positive large for any variable we would like to be small in the time domain [17]. In this robot system, the most important variable for the control is tilt angle, ϕ. Therefore, we have initially set $\mathbf{Q}$ and $\mathbf{R}$ the identity matrix and gave more weight to the diagonal term for ϕ for good performance. For small rising time and low overshoot for the overall control, $\mathbf{Q}$ was modified as in Equation (29) through

several simulations, and finally the feedback gain, **K** was computed in Equation (30) as follows:

$$\mathbf{Q} = \begin{bmatrix} 20 & 0 & 0 & 0 & 0 & 0 \\ 0 & 5 & 0 & 0 & 0 & 0 \\ 0 & 0 & 5 & 0 & 0 & 0 \\ 0 & 0 & 0 & 1 & 0 & 0 \\ 0 & 0 & 0 & 0 & 100 & 0 \\ 0 & 0 & 0 & 0 & 0 & 0.005 \end{bmatrix} \tag{29}$$

$$\mathbf{K} = \begin{bmatrix} -2.2361 & -3.2762 & 0.7071 & 0.7286 & -15.3874 & -2.1505 \\ -2.2361 & -3.2762 & -0.7071 & -0.7286 & -15.3874 & -2.1505 \end{bmatrix} \tag{30}$$

5.2. THE UPRIGHT BALANCING

The upright balancing is the most fundamental control for the two-wheeled inverted pendulum robot because no other control is possible without stable upright balancing. Maintaining the robot's upright balancing is similar to controlling a common inverted pendulum. However, the structure of the two-wheeled inverted pendulum robot is not identical to that of the widely known

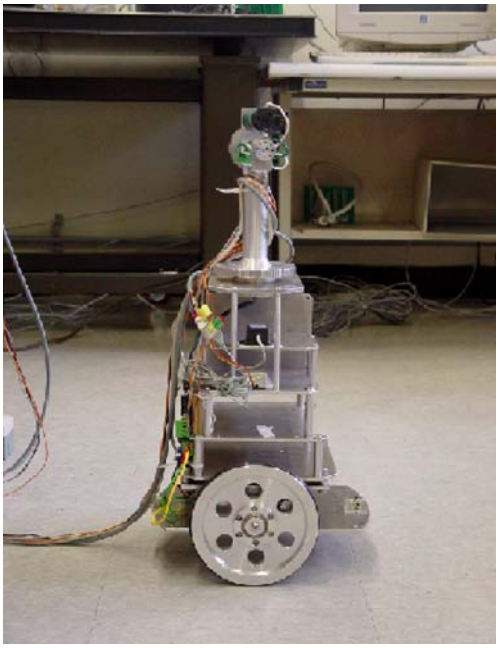

Figure 7. The upright balancing of the robot.

inverted pendulum. For instance, in a typical inverted pendulum, the inverted rod or body is connected to the base with a bearing that allows free rotation between the base and the upper pendulum; however, there is no bearing between the base and the upper body of the two-wheeled inverted pendulum robot. Consequently, free rotation occurs between the driving wheel and the upper body, which are connected without a bearing, though a gear box. Nonetheless, both cases of the two-wheeled inverted pendulum robot are more or less similar because, when no external force or torque is applied, the wheel turns around the axle and the upper body falls on the floor.

We used the upright balancing control for our robot, which had this structure or characteristic. For more stable operation, the robot should stay in the same position. The upright balancing enables the robot to keep its original position without losing its balance. In the initial condition, our robot was tilted 8° but the angular velocity of the tilt angle was zero.

We expected the robot to respond as follows: the initially tilted upper body is lifted up to 0°; the upper body has zero angular velocity around the wheels' axle; the center of the base remains at the original position; the base has no velocity in every direction; the steering angle and its time derivative remain zero. With these expectations, we conducted the simulation and experiment simultaneously. The feature of balancing experiment is shown in Figure 7 and the graphical results are shown in Figure 8.

As can be seen in Figure 8, the tilt angle of the mass center of the body and its time derivative cross the horizontal axis were within 0.25 s in both the simulation and the experiment. However, more than 3 s lapsed for the position of the center

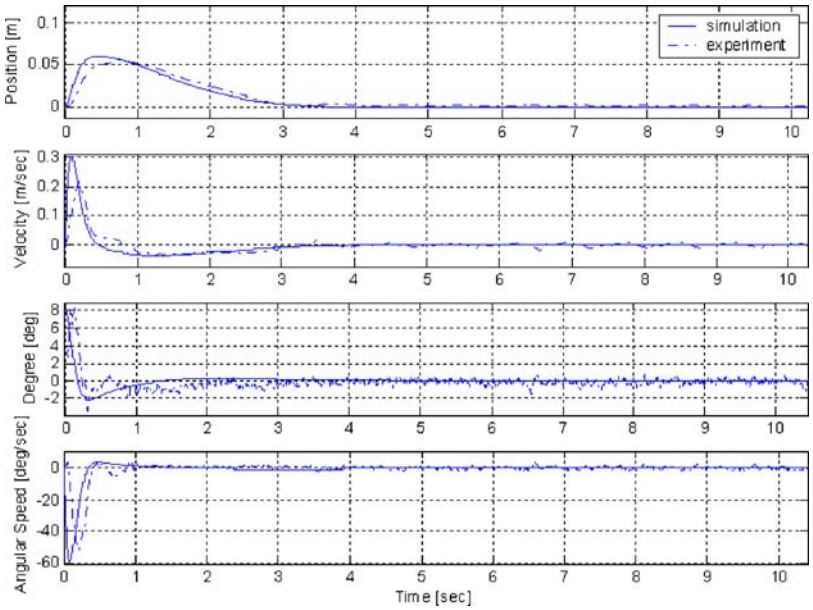

Figure 8. The experiment result: upright balancing.

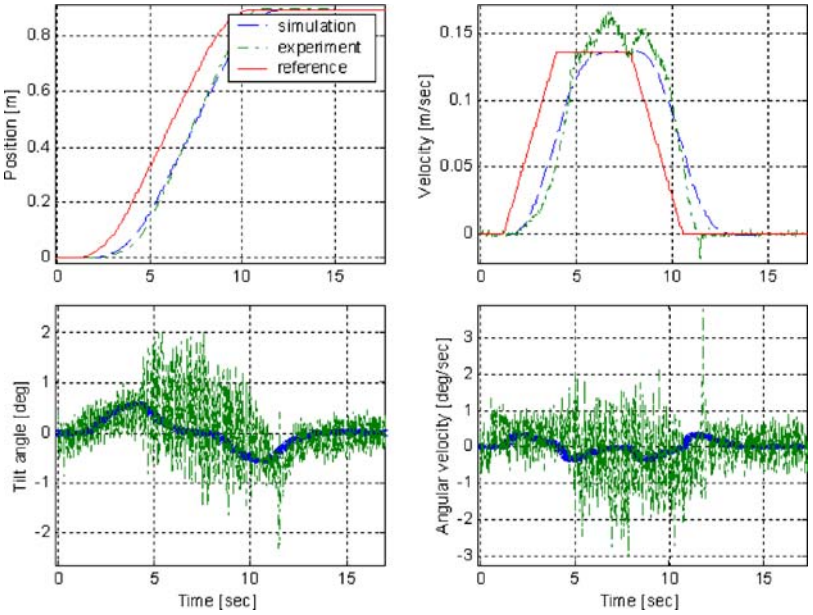

Figure 9. The experiment result: rectilinear motion.

of the base to return to its original position. Although there is a slight movement of the position to make the tilted body return to zero angle, the results are satisfactory and the upright balancing was successful.

At the same time, the results of the simulation agree well with the measurements of the experiment, even though there was a delay in the beginning for the position, velocity, tilt angle, and tilt angular velocity. The reason for the delay is that the initial condition was given in a slightly different way from the simulation. That is, the initial tilt angle was not exactly the same as in the simulation because the upper body was set to be tilted by human intervention. However, when the control started, the human intervention stopped and the robot's upper body was tilted more instantaneously at the beginning. The time taken for the balancing was much longer than the delay between the simulation and the experiment.

5.3. THE RECTILINEAR MOTION

With successful upright balancing control, we tried a more complicated motion such as a rectilinear motion. However, the initial condition for controlling a rectilinear motion is not the same as for upright balancing. That is, rectilinear motion starts and ends with a balanced upright condition. Instead of considering of the initial tilt angle, other facts had to be considered such as the reference profile of the position and the velocity of each drive wheel. Thus, the goal of the rectilinear motion control was to achieve exact agreement between the reference velocity and position profile and the experimental velocity and position profile.

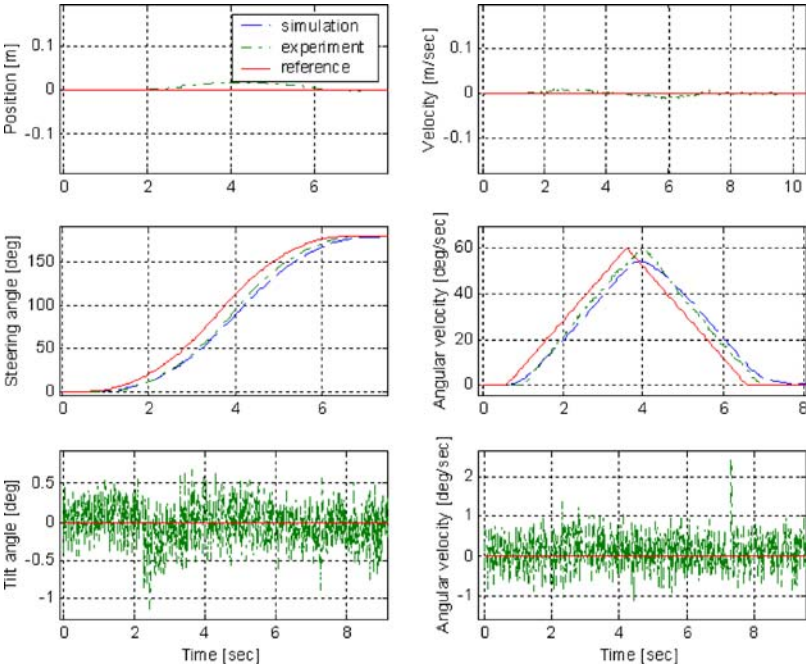

Figure 10. The experiment result: spinning motion.

To generate the reference velocity and position profile, we first generated the reference velocity profile and its integration was then used as the reference position profile. We then inputted the position of the right and left-drive wheels into the control system. Because no difference occurred between both wheels for the rectilinear motion control, the same position profile was given for both of wheels. Figure 9 shows the results. As can be seen in Figure 9, the rectilinear motion consists of the acceleration, constant velocity, and deceleration periods. Its position profile has a nonlinear *S* shape. Both the simulation and the experiment show a similar response but, after a few seconds had lapsed, they followed the reference profile because time is needed for the upper body to be inclined to move forward or backward.

The experiment and the simulation both showed the three elements of the velocity profile, namely, acceleration, constant velocity, and deceleration, to complete the rectilinear motion. The position and velocity had a delay between the reference and the response. The reasons for the error in simulated profile compared to the reference profile are mainly caused by the settling time for the position and velocity controls. As can be seen in the second graph of Figure 9, the reference profile has four corners of the trapezoidal shape, where the acceleration shifts suddenly. At those points, the robot needs settling time for the position and velocity controls, in amount about two seconds as shown in above two graphs of Figure 8. Nevertheless, the robot remained stable and the final position was the same as the reference. During the rectilinear motion, the tilt

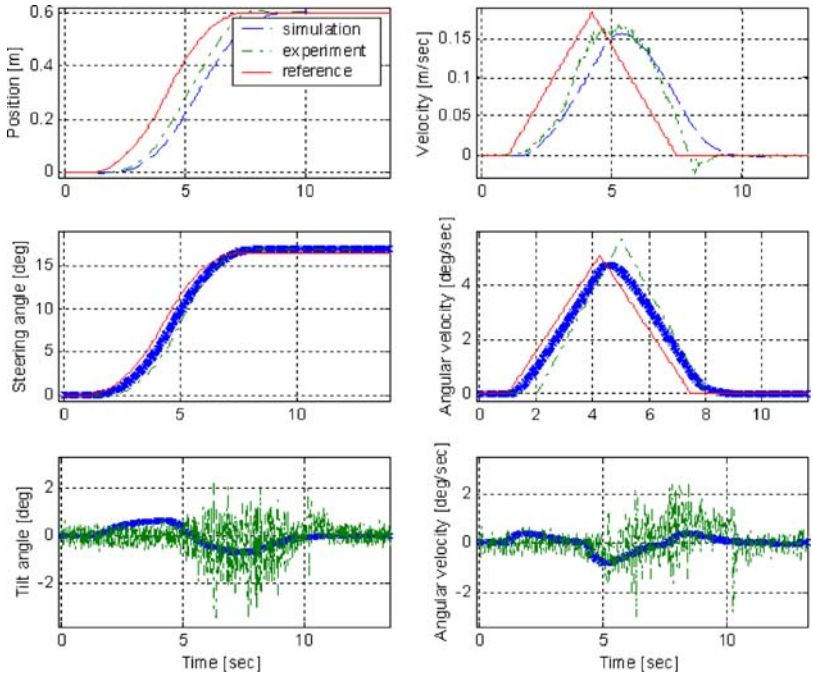

Figure 11. The experiment result: curvilinear motion.

angle and its time derivative were kept at zero for the stabilization of the robot, but they varied some degree in the simulation and in the experiment because the upper body could be moved without the body being tilted. Thus, the robot was slightly tilted forward and backward when it accelerated and decelerated, even though the constant velocity region remained zero.

5.4. THE SPINNING MOTION

To control the spinning motion, the same velocity reference profile with the opposite sign was applied to the two driving wheels. Based on the steering angular velocity profile, we generated the steering angle profile. As shown in Figure 10, the results of the simulation and the experiment agreed well with respect to the steering angle and its time derivative. Although an instantaneous deviation occurred in the position during the spinning motion, the robot recovered its original position.

For greater practicality, the robot needs to perform a more complicated motion. However, the robot can perform any motion by combining the unit motions realized above in 5.2, 5.3, and here. Finally, the robot was able to move to a desired position with a desired orientation. For example, a simple curvilinear motion was performed, as shown in Figure 11. This curvilinear motion was achieved using successful and stable unit motions such as the upright balancing motion, the rectilinear motion, and the spinning motion. The curvilinear motion

was consequently composed of the various characteristics of each unit motion already mentioned. In other words, time was needed for the robot to follow the reference position or velocity profile because the robot's upper body had to be tilted to enable it to move forward. Time was also needed for the robot to follow the steering angle or its velocity profile because the robot had to remain in the original position during the upright balancing while the upper body was being steered. These aspects are the unique characteristics of the two-wheeled inverted pendulum robot.

6. Conclusions

We proposed a two-wheeled inverted pendulum-type mobile robot as one style of home robot that could be used in the near future. It has the advantage of mobility from without caster and an innate clumsy motion for balancing. To analyze and execute this robotic mechanism, we used Kane's method of 3-DOF modeling to conduct an exact type of dynamic modeling. Using the governing equations of motion and simulation results, we analyzed the situation of an inclined surface and the effect of turning motion on the stability of the robot. The mechanical robot was constructed with three types of sensors: a gyroscope, a tilt sensor, and encoders. The applicability of our system to a two-dimensional surface in a home or office environment was confirmed by experiments on the balancing motion, rectilinear motion, and spinning motion. The 3-DOF dynamical modeling, along with our analysis and experiments on the two-wheeled inverted pendulum robot, should expedite the introduction of this kind of robot in real life.

References

1. Kitano, H., Okuno, H. G., Nakadai, K., Sabisch, T., and Matsui, T.: Design and architecture of SIG the humanoid, in: *Proceedings of the 2000 IEEE/RSJ International Conference on Intelligent Robots and Systems*, 2000, pp. 181–190.
2. Arkin, R. C., Fujita, M., Takagi, T., and Hasegawa, R.: Ethological modeling and architecture for an entertainment robot, in: *Proceedings of the 2001 IEEE International Conference on Robotics & Automation*, Seoul, Korea, 2001, pp. 453–458.
3. Ito, K., Matsuno, F., and Takahashi, R.: Underactuated crawling robot, in: *Proceedings of the 2000 IEEE/RSJ International Conference on Intelligent Robots and Systems*, 2000, pp. 1684–1689.
4. Alvarez-Gallegos, J. and Gonzalez-Hernandez, H. G.: Analysis of the dynamics of an underactuated robot: the forced pendubot, in: *Proceedings of the 36th Conference on Decision & Control*, San Diego, California, 1997, pp. 1494–1499.
5. Vilchis, J. C. A., Brogliato, B., Dzul, A., and Lozano, R.: Nonlinear modeling and control of helicopters, *Automatica* **39**(9) (2003), 1583–1596.
6. Au, S. K. W., Xu, Y., and Yu, W. W. K.: Control of tilt-up motion of a single wheel robot via model-based and human based controllers, *Mechatronics* **11** (2001), 451–473.
7. Awtar, S., King, N., Allen, T., Bang, I., Hagan, M., Skidmore, D., and Craig, K.: Inverted pendulum systems: rotary and arm-driven – a mechatronic system design case study, *Mechatronics* **12** (2002), 357–370.

8. Deniskina, I. V., Levik, Y. S., and Gurfinkel, V. S.: Relative roles of the ankle and hip muscles in human postural control in the frontal plane during standing, *J. Intell. Robot. Syst.* **27**(3) (2001), 317–321.
9. Yamajuji, K. and Kawamura, T.: Postural control of a monoaxial bicycle, *J. Robot. Soc. of Japan* **7**(4) (1989), 74–79.
10. Ha, Y. and Yuta, S.: Trajectory tracking control for navigation of the inverse pendulum type self-contained mobile robot, *Robot. Auton. Syst.* **17** (1996), 65–80.
11. Ambrose, R. O., Savely, R. T., Goza, S. M., Strawser, P., Diftler, M. A., Spain, I., and Radford, N.: Mobile manipulation using NASA's robonaut, in: *Proceedings of International Conference on Robotics and Automation*, New Orleans, Louisiana, 2004, pp. 2104–2109.
12. Thibodeau, B. J., Hart, S. W., Karuppiah, D. R., Sweeney, J. D., and Brock, O.: Cascaded filter approach to multi-objective control, in: *Proceedings of International Conference on Robotics and Automation*, New Orleans, Louisiana, 2004, pp. 3877–3882.
13. Browning, B., Rybski, P. E., Searock, J., and Veloso, M. M.: Development of a soccer-playing dynamically-balancing mobile robot, in: *Proceedings of International Conference on Robotics and Automation*, New Orleans, Louisiana, 2004, pp. 1752–1757.
14. Grasser, F., D'Arrigo, A., Colombi, S., and Rufer, A. C.: JOE: a mobile, inverted pendulum, *IEEE Trans. Ind. Electron.* **49**(1) (2002), 107–114.
15. Kane, T. R. and Levinson, D. A.: *Dynamics, Theory and Applications*, McGraw-Hill, 1985.
16. Greenwood, D. T.: *Classical Dynamics*, Prentice-Hall, New Jersey, 1997.
17. Dorato, P. and Abdallah, C.: *Linear–Quadratic Control, an Introduction*, Prentice-Hall, New Jersey, 1995.